ELSEVIER

Spectrochimica Acta Part B 63 (2008) 56–63

SPECTROCHIMICA ACTA PART B

www.elsevier.com/locate/sab

A Complementary Metal Oxide Semiconductor sensor array based detection system for Laser Induced Breakdown Spectroscopy: Evaluation of calibration strategies and application for manganese determination in steel

Fabiano Barbieri Gonzaga *, Celio Pasquini

Instituto de Química, Universidade Estadual de Campinas, Caixa Postal 6154, CEP 13084-971, Campinas/SP, Brazil

Received 11 June 2007; accepted 10 November 2007
Available online 17 November 2007

Abstract

This paper describes a low cost detection system for Laser Induced Breakdown Spectroscopy based on a simple spectrograph employing a conventional diffraction grating and a non-intensified, non-gated, non-cooled 1024 pixel Complementary Metal Oxide Semiconductor linear sensor array covering the spectral range from about 250 to 390 nm. It was employed in conjunction with a 1064 nm, 5 ns pulse duration Nd:YAG laser source for analyzing steel samples using the integration of 300 analysis pulses (35 mJ each). That led to gains in the signal-to-noise ratio of approximately 3 and 16 for Mn and Fe peaks, respectively, in addition to gains in the emission intensities of about 5.3, both in comparison with the integration of just 50 analysis pulses. The acquired emission spectra were used for Mn determination, in the range from 0.214 to 0.608% m/m as previously determined by ICP OES, evaluating different univariate (at different discrete wavelengths) and multivariate (over different spectral ranges) calibration strategies. The best results, using a PLS calibration model in the spectral range from 292.9 to 294.5 nm (related to Mn emission peaks), had relative errors of prediction of the Mn concentrations, for samples not employed in the calibration, from 0.3 to 7.3%, which are similar to or better than those obtained for Mn determination in steel using higher cost detection systems. The successful analytical application of the new detection system demonstrated that the performance of low cost detection systems can be very good for specific applications and that its low resolution and sensitivity can be at least partially compensated by the use of chemometrics and the integration of analysis pulses.

Keywords: LIBS; Detection system; PLS; Mn determination

1. Introduction

Laser Induced Breakdown Spectroscopy (LIBS) is an analytical technique based on the application of one or more high power short duration laser pulses on a reduced region of the sample to be analyzed, promoting its ablation and/or excitation, with the formation of a transient plasma, whose emitted radiation is monitored by means of an appropriate detection system (wavelength selector and detector) and is associated with the chemical composition of the sample. Although LIBS still presents some drawbacks in relation to other atomic spectroscopic techniques, mainly lower detectivity, advantages such as direct and fast analysis of practically any kind of sample (no need for sample pre-treatment or digestion procedures, allowing direct field analysis), lower sample consumption (practically non-destructive), and the possibility of micro-analysis (analysis of micro-regions of the sample, allowing analysis of solid surfaces with spatial resolution) make LIBS a very attractive analytical tool [1]. In addition, in recent decades, the development of modern solid state lasers (more compact and with shorter pulse duration), high resolution and wide spectral coverage polychromators, and highly sensitive gated detectors also contributed to the increase of interest in LIBS. Therefore, several reviews about this promising analytical technique have been published in the last few years [1–8].

In addition to the laser source, frequently a Q-switched Nd:YAG solid state laser [9–11], common LIBS instrumentation

* Corresponding author. Tel.: +55 19 35213037; fax: +55 19 35213023.
E-mail address: fbgalo@gmail.com (F.B. Gonzaga).

0584-8547/$ - see front matter © 2007 Elsevier B.V. All rights reserved.
doi:10.1016/j.sab.2007.11.005

also includes an optical system, to drive and focus the laser radiation onto the sample and to collect the radiation emitted by the plasma, a wavelength selector, such as an optical filter [12] or a grating polychromator, and a detector, such as a photomultiplier [13,14] (used to monitor discrete wavelengths) or a solid state sensor array. Recently, the use of a special kind of grating polychromator, called echelle polychromator, associated with an intensified charge coupled device containing a bi-dimensional sensor array (ICCD camera) has increased. The echelle polychromator, which employs two dispersing elements in a crossed configuration, generates a high resolution bi-dimensional dispersion covering a wide spectral range [15–17]. The ICCD camera employs an image intensifier (usually a micro-channel plate — MCP), which also acts as a fast radiation shutter, and a cooling device (a Peltier element) to increase sensitivity [18–20]. These features match the specific characteristics of plasma-emitted radiation: an initial high intensity background (eliminated by delaying MCP activation after the application of the laser pulse) superimposed on several low intensity atomic emission lines (some of them very close to each other). This makes the use of this kind of detection system almost compulsory in LIBS. However, as these components are very expensive and their dimensions impede their integration in portable instruments, conventional grating polychromators associated with non-intensified linear CCD [21,22] (without MCP) or intensified photodiode arrays [23,24] are still employed in LIBS instruments.

One of the interesting fields of LIBS applications has been the metallurgical industry, due to the need for fast and direct analysis of products, saving time and operating costs. Among the most analyzed samples, such as brass [25], gold [26], copper [27,28] and aluminum alloys [29,30], steel accounts for most LIBS applications [31–35], probably due to its wide industrial applications. In steel-making processes, some added elements, such as manganese, play an important role for improving the mechanical and chemical properties, such as strength, toughness and heat and corrosion resistance. Thus, the manganese content must be strictly controlled, since it contributes to determining the performance of steel materials, and a rapid and precise analytical method would be desirable [36]. In steel production, the final average manganese content is about 0.6% and the reproducibility of standard methods for manganese determination in steel range typically from 2 to 5% [37,38]. Although ICP OES, a well-established atomic emission spectroscopy technique, commonly has lower limits of detection and better accuracy and reproducibility than LIBS for elemental determinations, LIBS presents important advantages over ICP OES, as direct analysis of practically any kind of sample, practically non-destructive feature, possibility of micro-analysis, and others [1]. However, although LIBS is a high throughput analytical tool that can be applied for direct analysis of steel samples, its poor pulse-to-pulse energy repeatability [39–41], which affects spectral repeatability (and, therefore, precision and accuracy), and the high costs of some instrumental components, such as the echelle spectrograph and the ICCD camera, still restrict its wide application in the metallurgical industry.

The present paper describes a low cost detection system for LIBS, employing a conventional grating polychromator coupled to a non-intensified non-gated and non-cooled CMOS linear sensor array. The system was applied for manganese determination in steel samples, integrating the plasma radiation generated by the application of several analysis pulses and evaluating different calibration strategies, univariate and multivariate (using chemometrics), in order to compensate for pulse-to-pulse energy variations of the laser source and the low resolution and detectivity of the detection system.

2. Experimental

2.1. Instrumentation

The laser source employed was an actively Q-switched Nd:YAG laser (Quantel Brilliant) with 1064 nm wavelength, 360 mJ pulse energy, 5 ns pulse duration and 20 Hz pulse repetition rate. The laser pulses were driven and focused onto the sample surface using a dichroic mirror and a BK7 bi-convex lens. The lens position was adjusted so that its focus (25 cm) was located 0.5 cm below the sample surface. The focus position, also called beam waist position [42], was studied between 2 cm above and 2 cm below the sample surface, with the positions inside the sample giving higher signal-to-background ratios. In addition, for the analysis of steel samples using LIBS, the report of higher emission intensities with the focus below the sample surface is very common [43,44]. The plasma-emitted radiation was collected by means of a quartz bi-convex lens (short focal length), placed at 45° in relation to the sample surface and coupled to an optical fiber cable (50 μm core diameter), which was connected to the entrance of the home-made detection system. The detection system was composed of a Czerny–Turner grating polychromator, made using two concave mirrors (10 cm focus and 5 cm diameter) and a conventional holographic grating (Edmund Optics, 2.5 cm side, 1800 grooves mm^{-1}, 13° blaze angle), coupled to a 1024 pixel CMOS linear sensor array (Hamamatsu S8378-1024Q) and its driver circuit (Hamamatsu C9001). The detection system was arranged so that its spectral coverage was from approximately 250 to 390 nm along the sensor array (calculated using a Hg/Ar calibration source), giving a nominal resolution of 0.14 nm. A microcomputer containing a communication interface (ADLink PCI-9111) and running a home-made software (developed in Microsoft Visual Basic.Net 2003) was used to control the application of the laser pulses and for data acquisition from the detector. Schematic representations of the instrument and of the detection system are shown on Fig. 1.

2.2. Experimental procedure for Mn determination

LIBS spectra were obtained for 11 steel samples. The samples were pre-treated by polishing in order to remove surface contaminations. Each sample was analyzed in 3 replicates, each replicate by applying 300 laser pulses (35 mJ $pulse^{-1}$ — adjusted varying the laser Q-switch delay) at a different surface location, with the integration of the 300 generated plasmas by

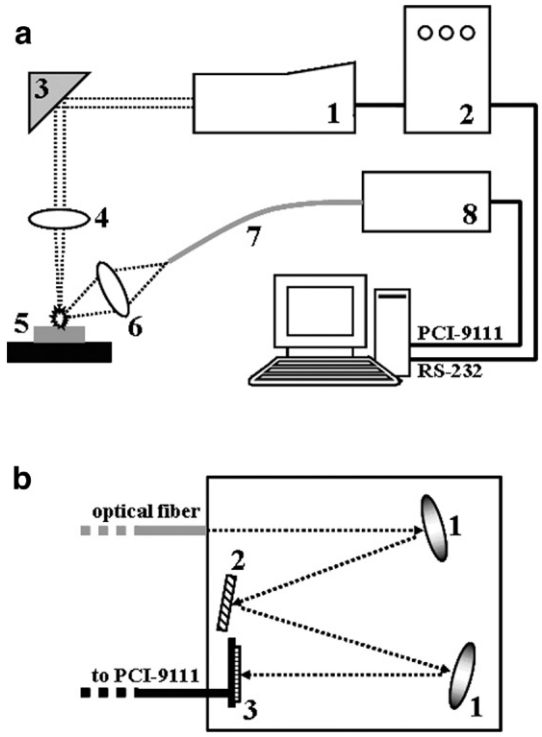

Fig. 1. (a) Schematic representation of the LIBS instrument: (1) Nd:YAG laser head, (2) laser control unit, (3) dichroic mirror, (4) laser focusing lens, (5) sample, (6) plasma collecting lens, (7) optical fiber cable, (8) detection system; (b) Schematic representation of the low cost detection system: (1) concave mirrors, (2) diffraction grating, (3) sensor array and its driver circuit.

the CMOS sensor array (15.5 s integration time gate). This pulse energy gave a theoretical irradiance of about 1.3×10^{10} W cm^{-2} pulse^{-1}, calculated according literature [42]. In the analysis of metal alloys, it was demonstrated that the lower the pulse energy, the lower the background emission [45] and that the non-gated detection can even lead to lower limits of detection than that obtained with gated detection when using lower pulse energies [46]. Therefore, a pulse energy much lower than the maximum provided by the laser was selected in order to avoid a higher background emission, once the detection here is non-gated. In addition with the use of a lower pulse energy, we have to use a higher number of analysis pulses in order to obtain a measurable emission spectrum, leading to a better repeatability of the emission signal (discussed later). The 3 spectra of replicates were averaged, giving just one LIBS spectrum representing each sample, and pre-treated by full multiplicative scatter correction (MSC) in order to correct baseline variations. Different calibration models were constructed and evaluated for Mn determination: some of them using univariate calibration based on peak heights at different wavelengths and others using multivariate calibration, by Partial Least Squares (PLS) with full cross validation, employing different spectral ranges. For all PLS models, the emission spectra were previously mean centered. The spectra of 6 or 7 samples (discussed later) were used for the construction of the calibration models for Mn concentration and the spectra of 4 samples (not used for calibration) were employed for predicting their Mn concentrations using the models constructed (external validation). The samples analyzed were secondary standard materials, whose Mn concentrations, determined by ICP OES, ranged from 0.214 to 0.608% m/m for 10 samples (distributed along the whole range). The remaining sample had 0.939% of Mn concentration. The average standard deviation of the Mn concentrations, evaluated by analyzing five replicates of three samples with different concentration levels, was determined as 0.008%. The PLS models were constructed using the software The Unscrambler 9.6 (CAMO, Norway).

3. Results and discussion

3.1. Integration of analysis pulses

The integration of all the radiation emitted from the plasmas generated by the application of several analysis pulses was necessary due to the low detectivity of the detector used; this integration substantially increased the emission intensity of LIBS spectra. Fig. 2a shows typical LIBS spectra obtained using the instrument developed for the same sample of steel, varying the number of analysis pulses from 50 to 300. For each spectrum obtained, the integration time gate of the detection system was adjusted according to the time necessary to integrate

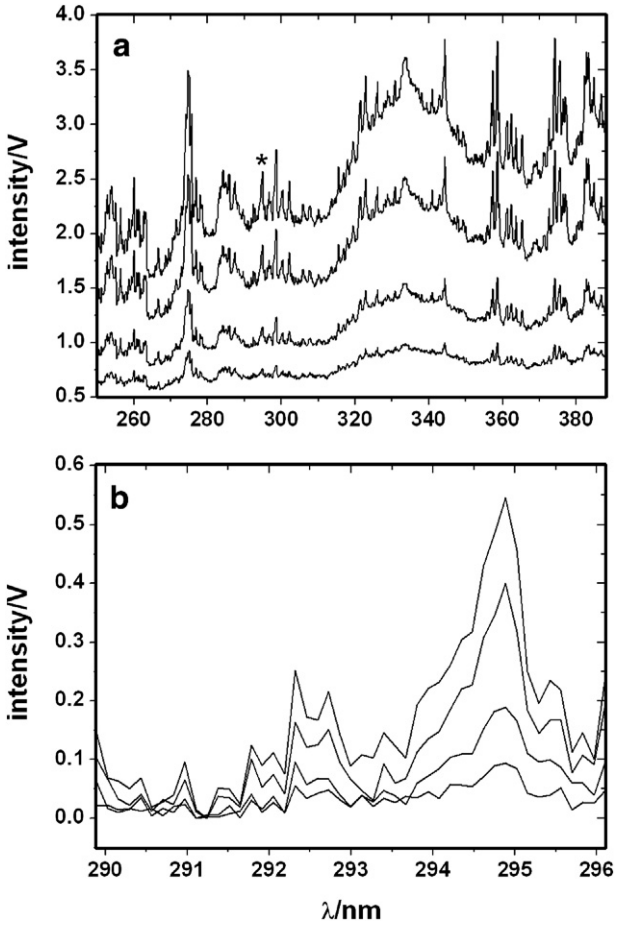

Fig. 2. Ordinary (a) and baseline corrected wavelength expanded (b) LIBS emission low resolution spectra for a steel sample using (from bottom to top) 50, 100, 200 and 300 analysis pulses.

the radiation emitted from all generated plasmas. Fig. 2b shows the same spectra, but with a zoom at the region of the Mn peak at 294.9 nm (identified with an asterisk in Fig. 2a) and baseline corrected, demonstrating the gain in the analytical signal with the increase of the number of analysis pulses.

3.2. Repeatability and signal-to-noise ratio

The relative low detectivity of the detection system required the integration of several analysis pulses in order to obtain an analytical signal with appreciable intensity. On the other hand, this analytical mode minimizes the pulse-to-pulse energy variation, leading to a better repeatability of the emission intensity and, consequently, to a better signal-to-noise ratio in the acquired LIBS spectra. A steel sample was analyzed in 5 replicates (at different surface locations) using 50 and 300 analysis pulses, in order to quantify these improvements. The acquired spectra were baseline corrected and 2 peaks having different wavelengths and intensity levels were analyzed: the Mn peak at 294.9 nm and the Fe peak at 344.3 nm.

The results, shown in Table 1, demonstrate gains of about 5.3 in the emission intensities, which are close to the expected factor of 6, when 300 analysis pulses were used in comparison with the use of 50 analysis pulses. The results also show gains of approximately 3 and 16 in the signal-to-noise ratios of the Mn and Fe peaks, respectively, which are also due to the improvement in the repeatability of the emission intensities with the increase in the number of analysis pulses. For the Mn line, although the relative standard deviation has also decreased, the decrease was lower than that for the Fe line, giving a lower increase factor in the signal-to-noise ratio. This might indicate a non-homogeneous distribution of the Mn in the samples, which is very common at these concentration levels. However, it is clear that the improvements when using 300 analysis pulses must be still higher in comparison with the use of just one analysis pulse, very common in analyses using LIBS.

As the highest emission intensities, repeatabilities and signal-to-noise ratios were obtained using 300 analysis pulses, that condition was used in all Mn determinations.

3.3. Mn determination

The determination of Mn in steel samples was evaluated employing different calibration models: univariate calibration models at discrete wavelengths related to Mn emission and multivariate calibration models using different spectral ranges.

Table 1
Effect of the number of analysis pulses on the signal-to-noise ratio of Mn and Fe emission peaks

λ/nm	Analysis pulses	Mean intensity/V	Standard deviation	RSD/% [a]	SNR [b]
294.9	50	0.100	0.019	19.00	5.26
	300	0.530	0.032	6.00	16.56
344.3	50	0.169	0.012	7.10	14.08
	300	0.909	0.004	0.44	227.25

[a] Relative standard deviation.
[b] Signal-to-noise ratio.

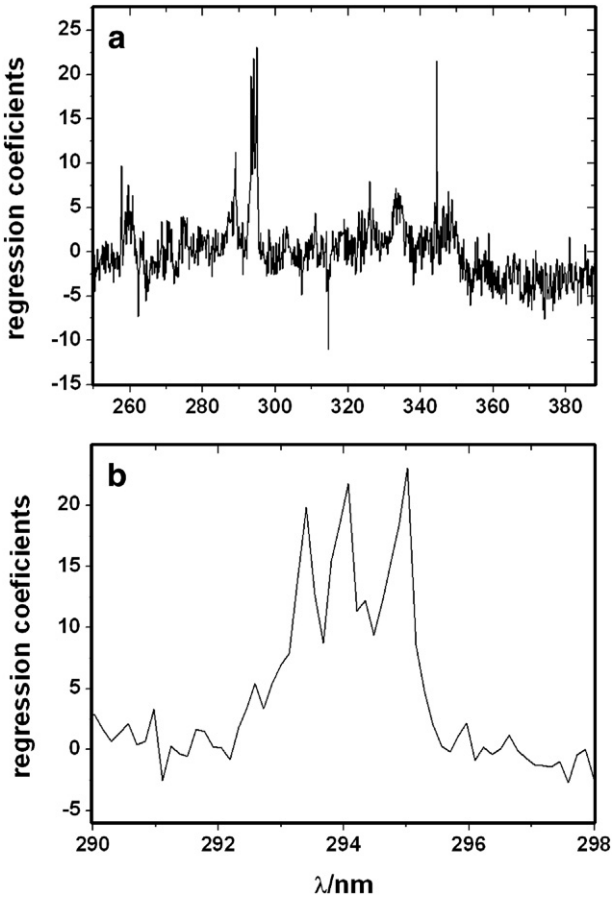

Fig. 3. Regression coefficients for a PLS calibration model using all emission spectra: (a) all the spectral range, (b) wavelength expanded showing maxima values related to Mn emission peaks.

For a preliminary investigation of the emission data, a PLS model for Mn concentration was constructed using all emission spectra. The regression coefficients using the first 2 latent variables, whose high values indicate the wavelengths of the emission spectra that best correlated to Mn concentrations, are shown in Fig. 3a. The spectral regions with the highest regression coefficients were those at about 294 nm and 344 nm, which are related to Mn and Fe emission peaks, respectively. The zoom at the spectral region from 290 to 298 nm, shown in Fig. 3b, revealed 3 regions of maxima regression coefficients, whose wavelengths are related to those of Mn emission peaks. Therefore, these 3 wavelengths were evaluated separately for Mn determination using univariate calibration.

Table 2 shows the results of the validation of the univariate models, using linear calibration, in predicting the Mn concentrations for 4 steel samples (not used in the construction of the model). For each wavelength, 2 calibration models were constructed: one employing the spectra of 6 samples, with Mn concentrations ranging from 0.214 to 0.608%, and the other employing 7 samples, including the sample containing 0.939% of Mn in order to evaluate the linearity of the models. The 4 validation samples were chosen in order to have samples with

Table 2
Results of Mn determination using different univariate calibration models

Calibration samples	λ/nm	R_{CAL} [a]	RMSEP [b]
6	293.4	0.961	0.028
	294.1	0.965	0.028
	295.0	0.911	0.078
7	293.4	0.970	0.042
	294.1	0.968	0.058
	295.0	0.941	0.105

[a] Correlation coefficient for the calibration.
[b] Root mean square error of prediction using external validation (in % m/m).

Mn concentrations homogeneously distributed in the range from about 0.2 to 0.6%, as in the calibration with 6 samples, as in the validation. The results showed better calibration and prediction for 293.4 and 294.1 nm, evaluated by means of higher correlation coefficients for the calibration and lower root mean square errors of prediction (RMSEP). The models with the sample containing 0.939% of Mn presented worse results, explained by their poorer linearities caused by including this sample, which might be due to the occurrence of some self absorption. Another source of errors in the models might be a non-homogeneous distribution of the Mn in the analyzed samples at the concentration levels studied, as discussed earlier.

Five different spectral ranges were used in the construction of the PLS models, employed for the evaluation of the Mn determination using multivariate calibration. One of them was the whole spectral range and the remaining ones were based on combinations of the wavelength ranges from 292.9 to 295.4 nm (related to Mn emissions) and from 344.3 to 344.7 nm (related to a Fe emission), both with the highest regression coefficients in the preliminary PLS model (Fig. 3a). Therefore, the 5 spectral ranges selected were: (i) all available wavelengths (from about 250 to 390 nm), (ii) 292.9 to 295.4 nm, (iii) 292.9 to 295.4 nm + 344.3 to 344.7 nm, (iv) 292.9 to 294.5 nm (covering just the 2 Mn emission peaks that presented best results using univariate calibration) and (v) 292.9 to 294.5 nm + 344.3 to 344.7 nm. The use of spectral ranges constituted those just by wavelength ranges related to Mn emissions and the same spectral ranges including also the wavelength range related to the Fe emission was made in order to evaluate the effect of the selection of a spectral range just by its regression coefficients (even if it was not related to the analyte) on the performance of the calibration models. The samples chosen for calibration and external validation were the same as for the univariate models and, in the same way, two calibration models were constructed for each selected spectral range: one including the sample containing 0.939% of Mn (7 calibration samples) and the other one without that sample (6 calibration samples). The results found for the calibration using full cross validation and external validation are shown in Table 3.

As can be seen, the use of 7 calibration samples led to models with a higher number of latent variables (LV), probably for trying to model non-linearities due to the inclusion of the sample containing 0.939% of Mn. In comparison with the corresponding models using 6 calibration samples, the models with 7 calibration samples almost always presented higher errors for predicting the Mn concentrations (RMSECV and RMSEP), explained, once more, by the poorer linearities caused by including the sample containing 0.939% of Mn, not successfully corrected by multivariate calibration models based on linear combinations, such as PLS. The same behavior was found for the univariate calibration models (in terms of RMSEP). The only exception is that for the multivariate calibration models using the spectral range from 292.9 to 295.4 nm, where the RMSEP for the model employing 7 calibration samples was a little lower than that employing 6 calibration samples, but using a higher number of latent variables, as discussed earlier, making it less robust. In addition, although we can see that the RMSECV values were, almost always, higher than the RMSEP values for a given spectral range and number of calibration samples, we can say nothing about the significance of that differences because of the low number of samples, as for the calibration (6 or 7 samples), as for the validation (4 samples).

Another important feature that can be seen is that calibration models including the spectral range related to Fe emission (344.3 to 344.7 nm) presented higher RMSEP, although they presented lower RMSECV, in comparison with the corresponding models employing just spectral ranges related to Mn emission peaks. That demonstrates that the wavelength selection for multivariate calibration using just the information of the regression coefficients (or the "loadings" data for the first principal components) from a preliminary data investigation, very common in chemometrics using other types of spectral data (such as those from near infrared spectroscopy), is not recommended for LIBS spectral data. LIBS spectra provide significant spectral information, characterized by several emission lines very close to each other (sometimes superimposed on each other). In addition, as expected concerning the previous explanation, the higher RMSECV and RMSEP values were obtained using the whole spectral range for the multivariate calibration. The excess of information present in the whole low

Table 3
Results of Mn determination using different multivariate calibration models

Calibration samples	λ/nm [a]	Calibration		Validation		LV [d]
		R_{PCV} [b]	RMSECV [c]	R_{PEV} [b]	RMSEP [c]	
6	All	0.231	0.150	0.986	0.046	2
	(1)	0.934	0.054	0.987	0.034	1
	(1)+(3)	0.940	0.053	0.986	0.036	1
	(2)	0.963	0.042	0.999	0.014	1
	(2)+(3)	0.978	0.036	0.998	0.022	1
7	All	0.776	0.143	0.897	0.063	3
	(1)	0.962	0.062	0.995	0.023	3
	(1)+(3)	0.982	0.046	0.978	0.041	2
	(2)	0.957	0.065	0.999	0.038	1
	(2)+(3)	0.984	0.042	0.939	0.058	2

[a] (1) 292.9–295.4; (2) 292.9–294.5; (3) 344.3–344.7.
[b] R_{PCV}: correlation coefficient between measured and predicted values using full cross validation; R_{PEV}: correlation coefficient between measured and predicted values using external validation.
[c] RMSECV: root mean square error of prediction using full cross validation; RMSEP: root mean square error of prediction using external validation (in % m/m).
[d] Number of latent variables used in the model.

resolution spectra, most of them not related to the manganese content, and the probable existence of several unresolved emission lines lead to worse calibration models. That demonstrates that, although the present detection system has a low cost, its low resolution imposes a caution against the abusive use of chemometrics. Therefore, the results of a preliminary multivariate data investigation serve as just a guide for wavelength selection, which must be made in conjunction with information about the atomic emission lines.

Finally, the best results for Mn determination, considering the RMSEP values, were obtained with the multivariate calibration model using 6 calibration samples and employing the spectral range covering just 2 (292.9 to 294.5 nm) of the 3 main Mn emission peaks from 292 to 296 nm, demonstrating the advantage of this kind of calibration over the simpler univariate calibration (much employed in LIBS). Further reduction of the spectral range in order to cover just one of the cited Mn emission peaks resulted in higher RMSEP values. Fig. 4 shows the LIBS spectra for the 6 calibration samples within the spectral range from 292 to 296 nm (showing a strong variation of the emission intensity mainly from about 292.9 to 295.4 nm due to the different Mn concentrations) and the predicted versus measured Mn concentrations graph for the calibration samples obtained with the best calibration model using full cross validation. The relative errors for Mn prediction ranged from about 0.3 to 7.3% for external validation using our best calibration model. Considering all samples (external validation and calibration with full cross validation), the average relative error for Mn prediction was about 7.0%. These values are similar to or better than those obtained for Mn determination in steel, within a similar concentration range, using LIBS with higher cost detection systems (polychromators with higher resolution and/or gated, cooled intensified detectors) [34,35]. For a future work, we can think of employing the present detection system for LIBS analysis of simpler matrices, as aluminum alloys, with a possible perspective of good results.

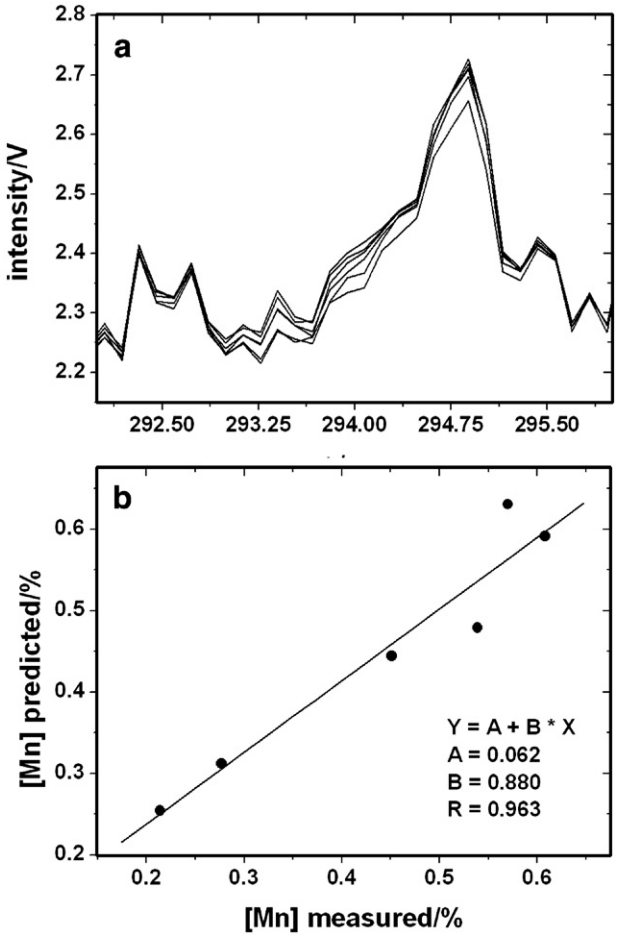

Fig. 4. (a) MSC corrected LIBS low resolution spectra for the calibration samples showing the variation of the emission intensity due to the different Mn concentrations; (b) plot of predicted versus measured Mn concentrations for the calibration samples obtained with the PLS model using the spectral range from 292.9 to 294.5 nm and full cross validation.

4. Conclusions

This paper has described a low cost detection system for LIBS, composed of a conventional grating polychromator coupled to a CMOS sensor array, whose development required a total cost of just US$ 700, which is much lower than the costs of gated and intensified detection systems usually employed in LIBS. In addition, this cost is also much lower than that of commercial low cost detection systems, as those from Ocean Optics, although this last one has a higher spectral resolution and sensitivity. Ocean Optics has a spectrograph for LIBS based on up to seven spectrographs, each one using a 2048 pixel linear CCD array and having a spectral coverage of 100 nm. The cost of each spectrograph is US$ 3674. The new detection system described here was successfully applied for Mn determination in steel samples using a Nd:YAG laser source for ablation and excitation.

The application of 300 analysis pulses of 35 mJ each and integration of the whole emitted radiation made possible the acquisition of emission spectra with good detectivity for the steel samples analyzed. The integration of several analysis pulses compensated the poor detectivity of the detection system by increasing the total emitted radiation measured and also minimizing the effect of pulse-to-pulse energy variation of the laser source and a possible non-homogeneous distribution of the Mn in the samples in terms of depth. The use of 300 analysis pulses led to gains in the signal-to-noise ratio of approximately 3 and 16 for Mn and Fe peaks, respectively, in addition to gains in the emission intensities of about 5.3, both in comparison with the application of just 50 analysis pulses.

Among the different univariate and multivariate calibration strategies evaluated for Mn determination using the acquired LIBS spectra, the best results were obtained using a PLS calibration model in the spectral range from 292.9 to 294.5 nm. This model had advantages in relation to the simple univariate calibration commonly used in LIBS, with relative errors of prediction of the Mn concentrations for 4 samples (not employed in the calibration) ranging from 0.3 to 7.3%. In addition, these results are similar to or better than those obtained for Mn determination in steel using higher cost detection systems, demonstrating that the use of multivariate calibration can also

compensate for the lower resolution and detectivity of lower cost detection systems. The results obtained with the different multivariate calibration models also showed the importance of selecting wavelengths for multivariate calibration using not only the regression coefficients, but also information about the relevant emission peaks.

Although the use of intensified and gated detectors in conjunction with high resolution polychromators has become almost compulsory in LIBS, the development of alternative detection systems for LIBS, such as that described in this paper, are very important in order to avoid the higher costs of the instrumentation related to this analytical technique, contributing to the dissemination of its application. In addition, as demonstrated in this paper, the performance of low cost detection systems can be very good for specific applications, where their lower resolution and detectivity can be at least partially compensated by the use of chemometrics and the integration of analysis pulses.

Acknowledgements

The authors are grateful to Dr. C. H. Collins for manuscript revision and to FAPESP for a post-doctoral scholarship and a research financing (process number 03/07419-5).

References

[1] C. Pasquini, J. Cortez, L.M.C. Silva, F.B. Gonzaga, Laser induced breakdown spectroscopy, J. Braz. Chem. Soc. 18 (2007) 463–512.
[2] J. Sneddon, Y. Lee, Novel and recent applications of elemental determination by laser-induced breakdown spectrometry, Anal. Lett. 32 (1999) 2143–2162.
[3] L.J. Radziemski, From LASER to LIBS, the path of technology development, Spectrochim. Acta Part B 57 (2002) 1109–1113.
[4] K. Song, Y. Lee, J. Sneddon, Recent developments in instrumentation for laser induced breakdown spectroscopy, Appl. Spectrosc. Rev. 37 (2002) 89–117.
[5] E. Tognoni, V. Palleschi, M. Corsi, G. Cristoforetti, Quantitative micro-analysis by laser-induced breakdown spectroscopy: a review of the experimental approaches, Spectrochim. Acta Part B 57 (2002) 1115–1130.
[6] J.D. Winefordner, I.B. Gornushkin, T. Correll, E. Gibb, B.W. Smith, N. Omenetto, Comparing several atomic spectrometric methods to the super stars: special emphasis on laser induced breakdown spectrometry, LIBS, a future super star, J. Anal. At. Spectrom. 19 (2004) 1061–1083.
[7] J.M. Vadillo, J.J. Laserna, Laser-induced plasma spectrometry: truly a surface analytical tool, Spectrochim. Acta Part B 59 (2004) 147–161.
[8] K. Song, Y. Lee, J. Sneddon, Applications of laser-induced breakdown spectrometry, Appl. Spectrosc. Rev. 32 (1997) 183–235.
[9] K. Tomiyasu, Laser bibliography — giant pulse techniques (Q-switching), IEEE J. Quantum Electron. 1 (1965) 144.
[10] A. Penzkofer, Solid-state lasers, Prog. Quantum Electron. 12 (1988) 291–427.
[11] R.L. Byer, Nonlinear optics and solid-state lasers: 2000, IEEE J. Sel. Top. Quantum Electron. 6 (2000) 911–930.
[12] D.N. Stratis, K.L. Eland, J.C. Carter, S.J. Tomlinson, S.M. Angel, Comparison of acousto-optic and liquid crystal tunable filters for laser-induced breakdown spectroscopy, Appl. Spectrosc. 55 (2001) 999–1004.
[13] R.E. Neuhauser, B. Ferstl, C. Haisch, U. Panne, R. Niessner, Design of a low-cost detection system for laser-induced plasma spectroscopy, Rev. Sci. Instrum. 70 (1999) 3519–3522.
[14] J.S. Huang, C.B. Ke, L.S. Huang, K.C. Lin, The correlation between ion production and emission intensity in the laser-induced breakdown spectroscopy of liquid droplets, Spectrochim. Acta Part B 57 (2002) 35–48.
[15] G.R. Harrison, The production of diffraction gratings: 2. The design of echelle gratings and spectrographs, J. Opt. Soc. Am. 39 (1949) 522–528.
[16] H.E. Bauer, F. Leis, K. Niemax, Laser induced breakdown spectrometry with an echelle spectrometer and intensified charge coupled device detection, Spectrochim. Acta Part B 53 (1998) 1815–1825.
[17] P. Lindblom, New compact Echelle spectrographs with multichannel time-resolved recording capabilities, Anal. Chim. Acta 380 (1999) 353–361.
[18] J. Janesick, G. Putnam, Developments and applications of high-performance CCD and CMOS imaging arrays, Annu. Rev. Nucl. Part. Sci. 53 (2003) 263–300.
[19] M. Sabsabi, V. Detalle, M.A. Harith, W. Tawfik, H. Imam, Comparative study of two new commercial echelle spectrometers equipped with intensified CCD for analysis of laser-induced breakdown spectroscopy, Appl. Opt. 42 (2003) 6094–6098.
[20] C. Haisch, H. Becker-Ross, An electron bombardment CCD-camera as detection system for an echelle spectrometer, Spectrochim. Acta Part B 58 (2003) 1351–1357.
[21] M. Sabsabi, R. Héon, L. St-Onge, Critical evaluation of gated CCD detectors for laser-induced breakdown spectroscopy analysis, Spectrochim. Acta Part B 60 (2005) 1211–1216.
[22] J.E. Carranza, E. Gibb, B.W. Smith, D.W. Hahn, J.D. Winefordner, Comparison of nonintensified and intensified CCD detectors for laser-induced breakdown spectroscopy, Appl. Opt. 42 (2003) 6016–6021.
[23] O. Samek, D.C.S. Beddows, H.H. Telle, J. Kaiser, M. Liska, J.O. Caceres, A.G. Urena, Quantitative laser-induced breakdown spectroscopy analysis of calcified tissue samples, Spectrochim. Acta Part B 56 (2001) 865–875.
[24] L. Burgio, K. Melessanaki, M. Doulgeridis, R.J.H. Clark, A. Anglos, Pigment identification in paintings employing laser induced breakdown spectroscopy and Raman microscopy, Spectrochim. Acta Part B 56 (2001) 905–913.
[25] G. Galbács, I.B. Gornushkin, B.W. Smith, J.D. Winefordner, Semi-quantitative analysis of binary alloys using laser-induced breakdown spectroscopy and a new calibration approach based on linear correlation, Spectrochim. Acta Part B 56 (2001) 1159–1173.
[26] M. Corsi, G. Cristoforetti, V. Palleschi, A. Salvetti, E. Tognoni, A fast and accurate method for the determination of precious alloys caratage by Laser Induced Plasma Spectroscopy, Eur. phys. j. D At. Mol. Opt. Phys. 13 (2001) 373–377.
[27] M. Sabsabi, P. Cielo, Quantitative-analysis of copper-alloys by laser-produced plasma spectrometry, J. Anal. At. Spectrom. 10 (1995) 643–647.
[28] F. Colao, R. Fantoni, V. Lazic, L. Caneve, A. Giardini, V. Spizzicchino, LIBS as a diagnostic tool during the laser cleaning of copper based alloys: experimental results, J. Anal. At. Spectrom. 19 (2004) 502–504.
[29] M.A. Ismail, H. Imam, A. Elhassan, W.T. Youniss, M.A. Harith, LIBS limit of detection and plasma parameters of some elements in two different metallic matrices, J. Anal. At. Spectrom. 19 (2004) 489–494.
[30] I.V. Cravetchi, M.T. Taschuk, Y.Y. Tsui, Evaluation of femtosecond LIBS for spectrochemical microanalysis of aluminium alloys, Anal. Bioanal. Chem. 385 (2006) 287–294.
[31] H. Balzer, S. Hölters, V. Sturm, R. Noll, Systematic line selection for online coating thickness measurements of galvanised sheet steel using LIBS, Anal. Bioanal. Chem. 385 (2006) 234–239.
[32] V. Sturm, J. Vrenegor, R. Noll, M. Hemmerlin, Bulk analysis of steel samples with surface scale layers by enhanced laser ablation and LIBS analysis of C, P, S, Al, Cr, Cu, Mn and Mo, J. Anal. At. Spectrom. 19 (2004) 451–456.
[33] C. Lopez-Moreno, K. Amponsah-Manager, B.W. Smith, I.B. Gornushkin, N. Omenetto, S. Palanco, J.J. Laserna, J.D. Winefordner, Quantitative analysis of low-alloy steel by microchip laser induced breakdown spectroscopy, J. Anal. At. Spectrom. 20 (2005) 552–556.
[34] K.Y. Yamamoto, D.A. Cremers, L.E. Foster, M.P. Davies, R.D. Harris, Laser-induced breakdown spectroscopy analysis of solids using a long-pulse (150 ns) Q-switched Nd: YAG laser, Appl. Spectrosc. 59 (2005) 1082–1097.
[35] J. Vrenegor, R. Noll, V. Sturm, Investigation of matrix effects in laser-induced breakdown spectroscopy plasmas of high-alloy steel for matrix and minor elements, Spectrochim. Acta Part B 60 (2005) 1083–1091.
[36] K. Wagatsuma, K. Kodama, H. Park, Precise determination of manganese in steel by dc glow discharge optical emission spectrometry associated with voltage modulation technique, Anal. Chim. Acta 502 (2004) 257–263.

[37] E. Truffaut, Manganese and historical development of the steel-industry, Rev. Metall-Paris 91 (1994) 1703–1719.
[38] ASTM E350-95 1995, Standard test methods for chemical analysis of carbon steel, low-alloy steel, silicon electrical steel ingot iron and wrought iron, ASTM, 1995, pp. 334–389.
[39] R.E. Russo, X.L. Mao, H.C. Liu, J. Gonzales, S.S. Mao, Laser ablation in analytical chemistry — a review, Talanta 57 (2002) 425–451.
[40] U. Panne, C. Haisch, M. Clara, R. Niessner, Analysis of glass and glass melts during the vitrification process of fly and bottom ashes by laser-induced plasma spectroscopy. Part I: normalization and plasma diagnostics, Spectrochim. Acta Part B 53 (1998) 1957–1968.
[41] J.M. Vadillo, I. Vadillo, F. Carrasco, J.J. Laserna, Spatial distribution profiles of magnesium and strontium in speleothems using laser-induced breakdown spectrometry, Fresenius' J. Anal. Chem. 361 (1998) 119–123.
[42] R. Noll, Terms and notations for laser-induced breakdown spectroscopy, Anal. Bioanal. Chem. 385 (2006) 214–218.
[43] M.A. Khater, J.T. Costello, E.T. Kennedy, Optimization of the emission characteristics of laser-produced steel plasmas in the vacuum ultraviolet: significant improvements in carbon detection limits, Appl. Spectrosc. 56 (2002) 970–983.
[44] C. Aragón, J.A. Aguilera, F. Peñalba, Improvements in quantitative analysis of steel composition by laser-induced breakdown spectroscopy at atmospheric pressure using an infrared Nd:YAG laser, Appl. Spectrosc. 53 (1999) 1259–1267.
[45] J.B. Sirven, B. Bousquet, L. Canioni, L. Sarger, Time-resolved and time integrated single-shot laser induced plasma experiments using nanosecond and femtosecond laser pulses, Spectrochim. Acta Part B 59 (2004) 1033–1039.
[46] G. Cristoforetti, S. Legnaioli, V. Palleschi, A. Salvetti, E. Tognoni, P.A. Benedetti, F. Brioschi, F. Ferrario, Quantitative analysis of aluminium alloys by low-energy, high-repetition rate laser-induced breakdown spectroscopy, J. Anal. At. Spectrom. 21 (2006) 697–702.